

Effect of Ag Doping on ZnO/V₂O₅ Nanoparticles as a Photo Catalyst for the Removal of Maxillion Blue (GRL) Dye

Ahmed Mesehour Ali Refaas^{1,2}, Enas M. AL-Robayi³ and Ayad F. Alkaim^{4*}

¹Department of Physics, College of Science, University of Babylon, Iraq

²Ministry of Education, Al-Muthana, Iraq

³Department of Physics, College of Science for Women, University of Babylon, Babylon, Iraq

⁴Department of Chemistry, College of Science for Women, University of Babylon, Babylon, Iraq

✉ alkaimayad@gmail.com

Received June 27, 2023; revised and accepted August 4, 2023

Abstract: In this research, the photo catalytic degradation of textile dyes as a model Maxillion Blue (GRL) dye by using Ag/ZnO/V₂O₅ nanocomposites synthesised via hydrothermal method. The physical properties of the as-synthesised nanocomposites were examined using characterisation techniques such as scanning electron microscopy (FE-SEM), energy-dispersive X-ray spectroscopy (EDX), TEM, and UV-vis spectroscopy. the production of pure ZnO, V₂O₅ nanoparticles and the discovery, by XRD analysis, of diffraction peaks related to the hexagonal phase of ZnO, V₂O₅, UV-vis spectroscopic calculations of the nanocomposite's energy bandgap (2.63 eV) indicated that it might function as a photo catalyst when exposed to UV-visible light. XRD also supported the fabrication of the ZnO/V₂O₅ nanocomposite. FE-SEM images showed that the object was spherical and somewhat hexagonal in form. EDX analysis reveals the presence of Zn, V, and O in the nanocomposite; its photocatalytic activity was evaluated through the degradation of GRL dye under exposure to solar light. The results showed that the optimum mass nanocomposite for efficient photo degradation was 0.4 g/L, with a degradation efficiency of 91.6%.

Key word: Textile dyes, zinc oxide, maxillion blue (GRL), hydrothermal, photo catalyst, nanoparticles.

Introduction

Environmental contamination is a problem that is getting more and more serious today. In this regard, the photocatalytic technology, which aims to decompose the organic materials discharged in the atmosphere, offers a fresh idea for the preservation and restoration of the environment. ZnO is one of the most effective semiconductor photocatalysts due to its benefits including quick response, full degradation, consistent performance, mild reaction conditions, and low cost. More importantly, ZnO has great potential for the breakdown of organic materials and is devoid of toxicity

and secondary contamination. In particular, ZnO has a huge surface area when it exists as nanoplatelets, which offers a lot of photocatalytic sites, a lot of electrode-electrolyte contact regions, a short diffusion path, and a fast transport rate (Aljeboree et al., 2019; Hashim et al., 2019). Additionally, it possesses great mechanical toughness and enough free volume, which are crucial for reducing structural stress brought on by the photocatalysis process. ZnO has two drawbacks as a single photocatalyst, though: (1) ZnO has a low quantum yield due to its quick electron-hole recombination. (2) Due to its large band gap, ZnO can only be activated by UV, which results in a low utility of solar energy

*Corresponding Author

since UV only makes up 3-4% of sunlight. Therefore, the effective improvement of ZnO quantum yield and the expansion of ZnO's absorption spectrum to the visible light region have emerged as major research areas (Jamil et al., 2018; Mosaa et al., 2019). Noble metal deposition and oxide semiconductor hybridization are generally acknowledged as two effective techniques. Oxide semiconductor hybridization is a technique that combines two distinct semiconductors for a beneficial outcome. The circular movement of the photo-generated electrons and holes between the two semiconductors has the potential to extend carrier lifespan, widen the absorption spectrum and improve the efficiency of solar energy. For instance, V_2O_5 is an oxide semiconductor with a small (2.80 eV) band gap. As a result, the absorption spectrum can be widened to include the visible light area through the hybridisation of ZnO with V_2O_5 (Algubili et al., 2015).

However, it has been discovered that the presence of low-valence vanadium ions leads to the formation of impurities that reduce the band gap. Additionally, the oxygen vacancies created by the lattice flaws act as the centers for the electron-hole pairs to be trapped, which promotes their quick recombination and hinders the successful destruction of the organic material. A significant difficulty in this area is figuring out how to prevent recombination and increase the lifetime of the electron-hole pairs (Karam et al., 2015).

On the other hand, due to the surface plasmon resonance, the deposition of a noble metal (such as Ag) can achieve significant visible light absorption and effectively separate the electron-hole pairs. The development of delicate ternary nanostructures made of co-doped Ag and V_2O_5 nanoplatelets is a highly intriguing idea, and by doing so, we hope to attain higher photocatalytic activities, particularly in the visible light area, through an amazing synergistic effect. To the best of our knowledge, hierarchical assembly does not offer a straightforward method for creating delicate ternary nanostructures. In our earlier study, we revealed a simple method for the hierarchical assembly of low-dimensional entities on two-dimensional nanoplatelets based on van der Waals interactions (Al-Gubury et al., 2015). Here, we describe fragile ternary nanostructures made of co-doped ZnO nanoplatelets, Ag, and V_2O_5 nanoparticles for the first time. This systematically investigated process forms a connection between composition and photocatalytic performance. We discovered a striking synergistic relationship between the three elements, providing a solid foundation for the creation of high-performance, next-generation composite photocatalysts.

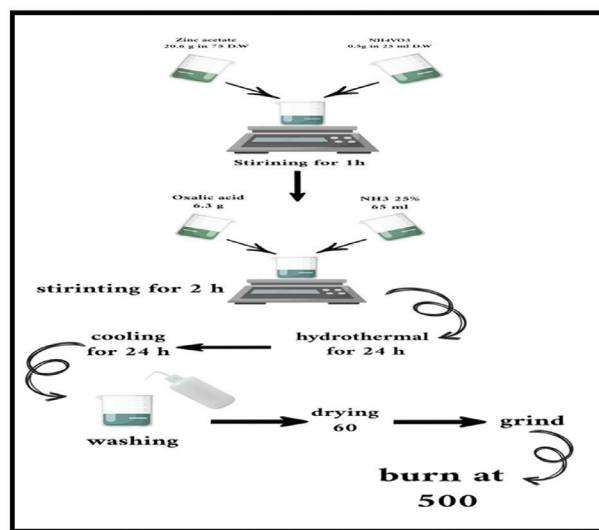
Experimental Part

Materials

Maxillion Blue (GRL) dye was created using ammonium metavanadates (NH_4VO_3), zinc acetate, oxalic acid, ethanol C_2H_5OH , and aqueous ammonia (25%) that were all acquired from Sigma-Aldrich in Germany. In order to get 100 mg/L of GRL dye in double-distilled water, a standard solution of 0.1g in 1000 mL was prepared.

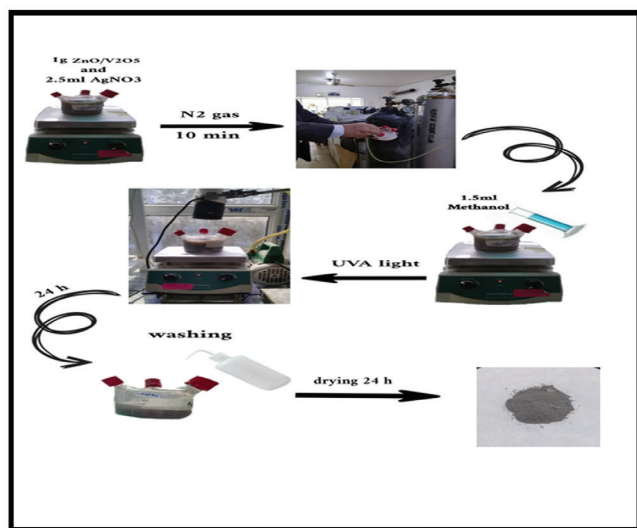
Preparation of Silver (Ag) Doped ZnO/ V_2O_5 Nanocomposites

Ammonium metavanadates (NH_4VO_3) were thermally hydrolysed to prepare ZnO/ V_2O_5 nanoparticles, and the experiment was conducted in a 150 mL teflon cup housed inside a stainless steel autoclave. In each experiment, 75 mL of an aqueous zinc acetate solution (20.6 gm zinc acetate, 75 mL water) was added to 25 mL of ammonium metavanadates (0.5 gm NH_4VO_3 , 25 mL water), and the mixture was thoroughly stirred for an additional 60 minutes. The mixture was then thoroughly stirred for a further 120 minutes before the addition of 6.3 g of oxalic acid and 65 mL of 25% aqueous ammonia. The finished product was then poured into a teflon cup. After the Teflon cup was sealed within the autoclave, it was shut off and placed into an electric furnace that was kept at 160°C for 24 hours. After the autoclave had finally cooled to room temperature, the powder was separated by centrifuging it repeatedly (at least three times) at 6000 rpm. It had also been washed with cold water at least four times and had been dried overnight in a 60°C oven, as shown in Scheme (1).



Scheme 1: Preparation of ZnO/ V_2O_5 nanoparticles.

The silver Ag that was deposited on the ZnO/V₂O₅ nanoparticle was created by placing 0.5g of ZnO/V₂O₅NPs and 1.5 ml AgNO₃ in a quartz cell. Next, the system was upregulated by N₂ (nitrogen gas) for 5 minutes before being exposed to UVA light (wavelength 365 nm and light intensity of 1.71mW/cm²) while being continuously stirred for 24 hours. To obtain the nanoparticles, the resultant powder was dried for 24 hours at 60°C and repeatedly rinsed with deionized water. Scheme (2) depicts a real-world image of silver being deposited onto ZnO/V₂O₅ nanoparticles.



Scheme 2: Preparation of silver(Ag) doped ZnO/V₂O₅ nanocomposites.

Result and Discussion

Characterisation of Nanocomposite

This technique is used to study the shape and structure of the surface and to study the particle size rate of the Ag/ZnO/V₂O₅ nanocomposite by means of a beam of high-energy electrons with an acceleration voltage of 200 KV.

Figure 1 shows TEM images of Ag/ZnO/V₂O₅, where the nanoparticles were observed, and it is noted that the spherical silver particles are well distributed on the surface of ZnO. A clear variation was observed in the spacing between the tips of the zinc oxide and the silver particles, and with crystal sizes of 200 nm, 100 nm and 60 nm, the zinc oxide nanoparticles were embedded inside the silver and vanadium (Abd et al., 2020).

Figure 2 shows that very high agglomeration results in better dispersion of the FE-SEM image. It was determined from XRD crystalline size data and SEM images that all Ag/ZnO/V₂O₅ produced had tiny nanoparticles crystallised (Alkaim and Ajobree, 2020; Bader et al., 2019). SEM measurements, however, provide a complete concordance with the crystal size determined by XRD measurements.

Because of the poor crystallinity, ZnO/V₂O₅ exhibits the agglomeration phase. Additionally, the results demonstrate that the Ag/ZnO/V₂O₅ sample is homogeneous in terms of size and shape. The huge specific surface area and high surface energy of Ag/

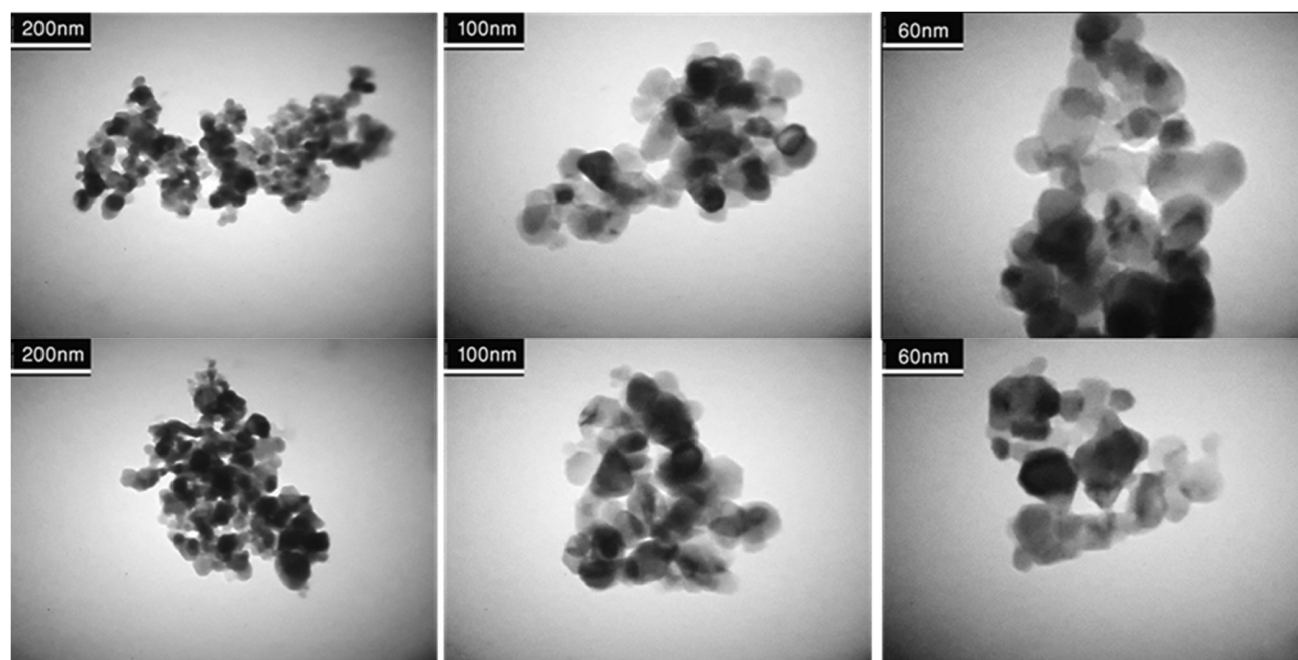


Figure 1: TEM images of Ag/ZnO/V₂O₅ nanoparticle.

ZnO/V₂O₅ nanoparticles should have been the source of the particle aggregation (or production of bigger particles). Ag/ZnO/V₂O₅ nanoparticles thus severely agglomerate as a result of the high surface energy and large specific surface area. Studying FE-SEM micrographs reveal fewer pores and smaller lumps, which would cause particles to behave differently and form nanorode forms rather than spindle particles (Abass et al., 2018; Abd et al. 2020).

X-ray diffraction (XRD) pattern of ZnO shows no other summit, indicating the presence of the impurity. This is an indication that these nanoparticles of zinc

oxide possess one phase. The impurity patterns were observed due to the effect of calcination. Nine peaks appear at 31.7°, 34.4°, 36.2°, 47.5°, 56.5°, 62.82°, 66.4°, 67.9° and 69.10°, which correspond to the (100), (002), (101), (102), (110), (103), (200), (112) and (201), reflection planes, in the same order (Abdulrazzak, 2016; Abdulrazzak et al., 2021). All the peaks diffraction can also be suggested to the hexagonal wurtzite structure of ZnO JCPDS card (no. 36-1451) and phase pure with the result a highly crystalline due to very sharp and strong peaks as shown in Figure 3a.

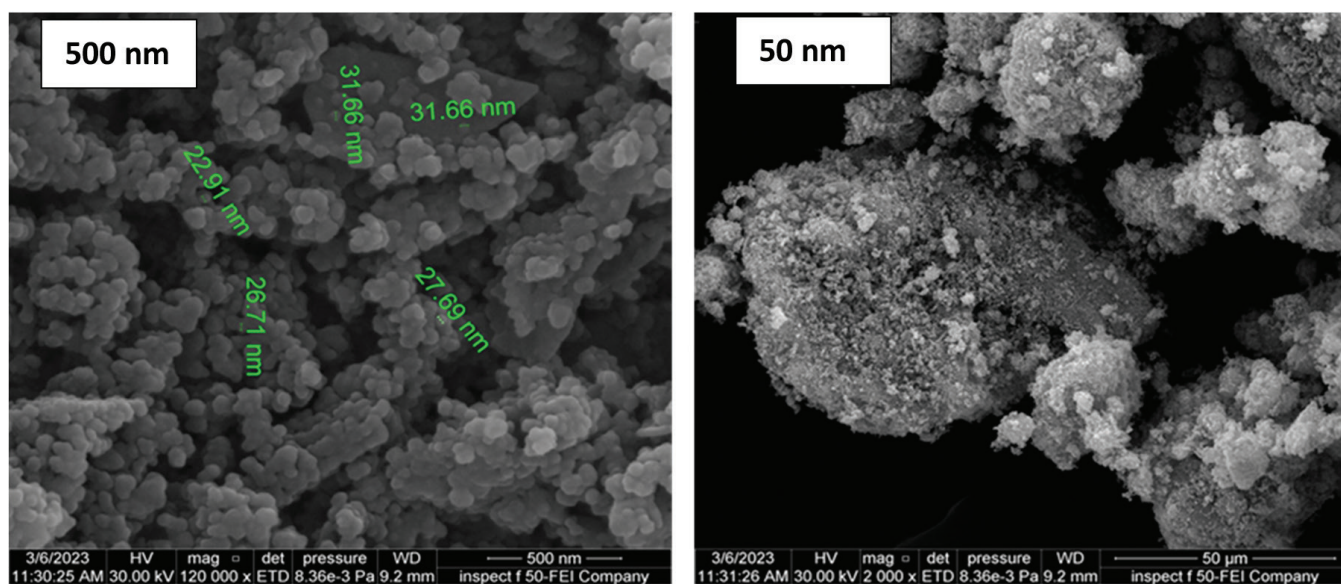


Figure 2: FE-SEM images of Ag/ZnO/V₂O₅ nanocomposite.

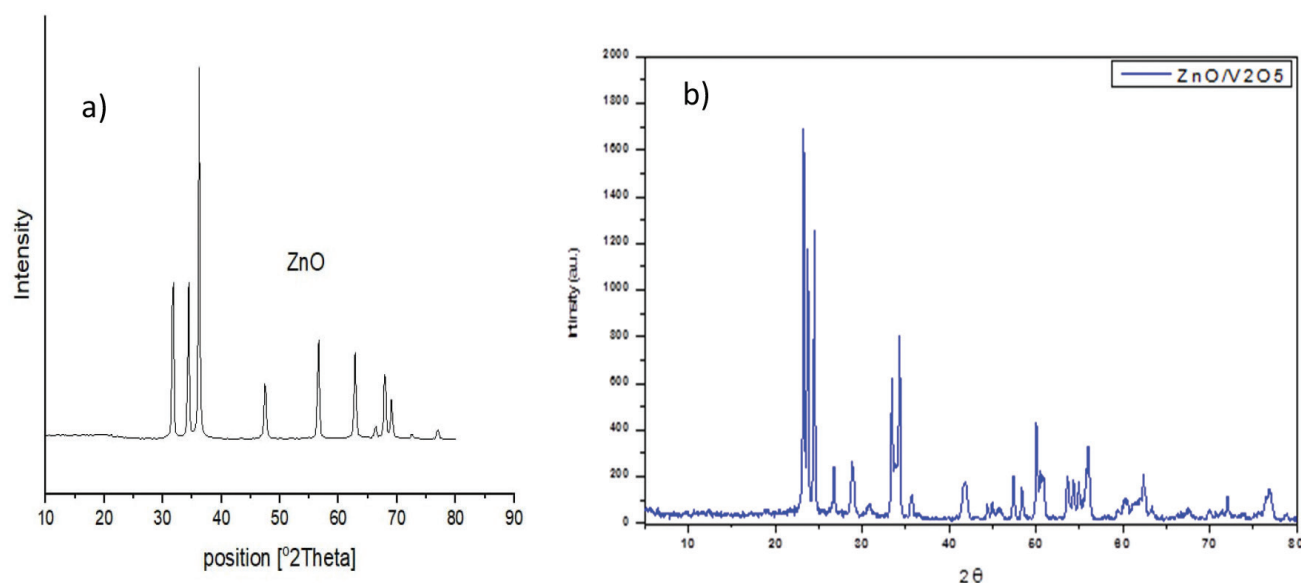


Figure 3: X-ray diffraction patterns of (a) ZnO and (b) ZnO–V₂O₅ nanocomposite.

The phase stability and phase transition of the ready catalysts, V₂O₅, were investigated using XRD. Figure 6 displays the outcomes of employing the full width at half maximum (FWHM). Based on the peak width (B), one may calculate the particle size (P), which yields a shape factor (k) of 0.9, a wavelength of the x-ray source of 0.1541 nm, and a B value for the whole peak width at half maximum corrected for instrumental broadening (Khedaer et al., 2021). The XRD pattern of the synthesised catalyst is shown in Figure 3b. One type of phase is well indexed to V₂O₅ with an orthorhombic structure. The other type of phase is known to exist in ZnO hexagonal structure. This XRD pattern revealed no further possible impurities, such as VO₃ and V₂O₃, indicating that the final product solely contained the distinct diffraction peaks of V₂O₅ and ZnO (Abdulrazzak et al., 2021; Ali et al., 2019; Hashim et al., 2019).

Effect of Mass Dosage

Effect of quantities (0.1, 0.2, 0.4, and 0.6 gm) of Ag/ZnO/V₂O₅ nanocomposite on the photocatalytic degradation of (GRL) dye at a reaction temperature of 25°C for a period of one hour. The analysis of first order experimental data is depicted in Figure 5. The effect of adsorbent dosage on the removal of 10 mg/L GRL dye. After one hour, the PDE% increased by [60.089 - 71.068]% due to the Ag/ZnO/V₂O₅ NPs' rising weight of around 0.1-0.6 gm (Abdulrazzak et al., 2019; Ali et al., 2019).

Effect of Concentration of GRL Dye

To examine the impact of the initial GRL dye concentration on Ag/ZnO/V₂O₅ nanocomposite, many

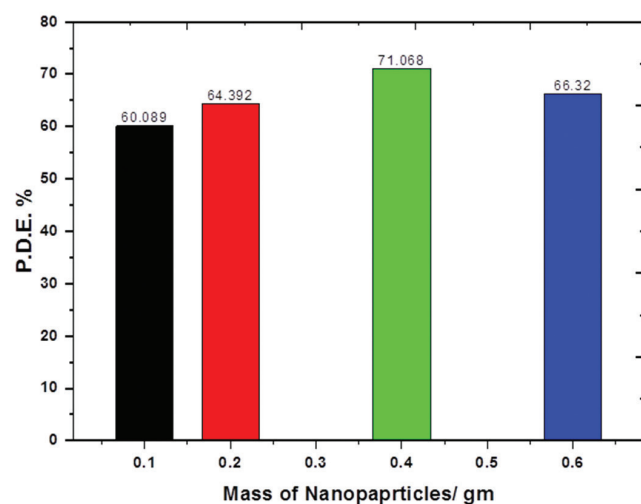


Figure 4: Effect of photo degradation efficiency of GRL at several dosages.

dye concentrations (4–25 mg/L) were chosen for this study. The amounts of GRL adsorbed at solution pH 6 are depicted in Figure 6 as 0.6 g of Ag/ZnO/V₂O₅ nanocomposite. GRL dye solution is essential for estimating the rate of photocatalytic degradation as well as the time dependency of this process at various concentrations. Assuming first-order kinetics based on the experimental results, Figure 5 shows first-order kinetics. After 1 hour of adsorption, the elimination percentage increased by [91.03-16.37]% as the GRL dye concentration increased by roughly 2 to 25 ppm (Abdulrazzak and Hussein, 2018; Abdulrazzak et al., 2021).

Effect of Light Intensity (L.I.)

By varying the distance between the light source and the material's exposed surface, the influence of light intensity (0.8-2.6 mW/cm²) was seen. GRL dye photo

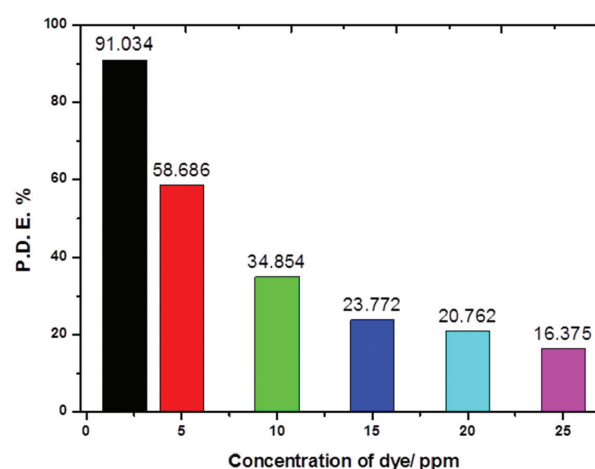


Figure 5: Photocatalytic degradation of GRL at several concentrations.

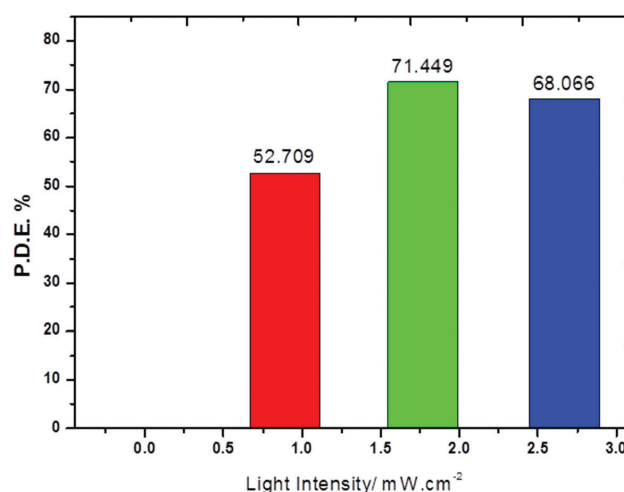


Figure 6: Effect of light intensity onto photocatalytic degradation of GRL dye.

degradation under the effect of L.I. was examined in 0.4 g of Ag/ZnO/V₂O₅ nanocomposite with a GRL dye concentration of 10 mg/L. All reactions were found to proceed in accordance with the first-order kinetics shown in Figure 6. The rate of photocatalytic degradation and PDE% increased with increasing UV intensity light since more radiation is available to excite the catalyst and, as a result, more charge carriers are produced (Mashkour et al., 2011).

Conclusion

The hydrothermal method was successfully used to prepare ZnO/V₂O₅ nanocomposite and enhanced the surface by using the photo deposition method of silver metal to prepare Ag/ZnO/V₂O₅. The effect of light intensity plays a good role in increasing surface activity while when the concentration of aqueous dye increases the activity of the surface reduces as a photocatalyst. We conclude the prepared surface has good photo-catalytic activity for degradable aqueous pollutants.

References

- Abass, K.H., Shinen, M.H. and A.F. Alkaim (2018). Preparation of TiO₂ nanolayers via sol-gel method and study the optoelectronic properties as solar cell applications. *Journal of Engineering and Applied Sciences*, **13(22)**: 9631-9637.
- Abd, I.K., Abdulrazzak, F.H. and Z.T. Khodair (2020). Synthesis of MWCNTs from methanol/butanol mixture by catalytic chemical vapor deposition and application to synthesized dye sensitizer solar cell. Paper presented at the 2nd International Conference on Materials Engineering and Science, University of Technology Baghdad-Iraq.
- Abdulrazzak, F.H. (2016). Enhance photocatalytic activity of TiO₂ by carbon nanotubes. *International Journal of ChemTech Research*, **9(3)**: 431-443.
- Abdulrazzak, F.H., Abbas, A.M. and F.H. Hussein (2019). Synthesis of multi-walled carbon nanotubes from Iraqi natural gas/Co mixture by catalytic flame fragments deposition method. *Asian Journal of Chemistry*, **31(1)**: 247-250.
- Abdulrazzak, F.H. and F.H. Hussein (2018). Photocatalytic hydrogen production on nanocomposite of carbon nanotubes and TiO₂. *Journal of Physics: Conference Series*, **1032**: 012056.
- Abdulrazzak, F.H., Jawad, M.A., Alkadir, O.K.A. and A.F. Alkaim (2021). Antimicrobial activity of Ag:ZnO/MWCNT against *Cinetobacter baumannii*. *Journal of Nanostructures*, **11(2)**: 317-322.
- Abdulrazzak, F.H., Jimaa, R.B., Radhi, I.M. and T.A. Himdan (2021). XRD and microscopic images for synthesis graphite nanoparticles by oxidation method. *NeuroQuantology*, **19(2)**: 45-49.
- Al-Gubury, H.Y., Fairouz, N.Y., Aljeboree, A.M., Alqaraguly, M.B. and A.F. Alkaim (2015). Photocatalytic degradation n-undecane using coupled ZnO-Co₂O₃. *International Journal of Chemical Sciences*, **13(2)**: 863-874.
- Algubili, A.M., Alrobayi, E.M. and A.F. Alkaim (2015). Photocatalytic degradation of remazol brilliant blue dye by ZnO/UV process. *International Journal of Chemical Sciences*, **13(2)**: 911-921.
- Ali, R., Radhi, I.M., Ismail, A.A. and F.H. Abdulrazzak (2019). Modified ZnO for efficient photo-catalysis by Silver/Graphite oxide nanoparticles. *Journal of Global Pharma Technology*, **11(7)**: 143-150.
- Aljeboree, A.M., Alshirifi, A.N. and A.F. Alkaim (2019). Activated carbon (as a waste plant sources)-clay micro/nanocomposite as effective adsorbent: Process optimization for ultrasound-assisted adsorption removal of amoxicillin drug. *Plant Archives*, **19**: 915-919.
- Alkaim, A.F. and A.M. Ajobree (2020). White marble as an alternative surface for removal of toxic dyes (methylene blue) from aqueous solutions. *International Journal of Advanced Science and Technology*, **29(5)**: 5470-5479.
- Bader, A.T., Zaied, A.M. Aljeboree, A.M. and A.F. Alkaim (2019). Removal of methyl violet (MV) from aqueous solutions by adsorption using activated carbon from pine husks (plant waste sources). *Plant Archives*, **19**: 898-901.
- Hashim, F.S., Alkaim, A.F., Mahdi, S.M. and A.H. Omran Alkhayatt (2019). Photocatalytic degradation of GRL dye from aqueous solutions in the presence of ZnO/Fe₂O₃ nanocomposites. *Composites Communications*, **16**: 111-116.
- Hashim, F.S., Alkaim, A.F., Salim, S.J. and A.H.O. Alkhayatt (2019). Effect of (Ag, Pd) doping on structural, and optical properties of ZnO nanoparticles: As a model of photocatalytic activity for water pollution treatment. *Chemical Physics Letters*, **737**: 136828.
- Jamil, D. M., Al-Okbi, A.K., Hanon, M.M., Rida, K.S., Alkaim, A.F., Al-Amiery, A.A., Kadhim, A. and A.H. Kadhum (2018). Carboxythiazole corrosion inhibitor: As an experimentally model and DFT theory. *Journal of Engineering and Applied Sciences*, **13(11)**: 3952-3959.
- Karam, F.F., Kadhim, M.I. and A.F. Alkaim (2015). Optimal conditions for synthesis of 1, 4-naphthoquinone by photocatalytic oxidation of naphthalene in closed system reactor. *International Journal of Chemical Sciences*, **13(2)**: 650-660.
- Khedaer, Z., Ahmed, D.S. and S.M.H. Al-Jawad (2021). Investigation of morphological, optical, and antibacterial properties of hybrid ZnO-MWCNT prepared by sol-gel. *Journal of Applied Sciences and Nanotechnology*, **1(2)**: 66-77.

Mashkour, M.S., Al-Kaim, A.F., Ahmed, L.M. and F.H. Hussein (2011). Zinc oxide assisted photocatalytic decolorization of reactive red 2 dye. *International Journal of Chemical Sciences*, **9(3)**: 969-979.

Mosaa, Z.A., Bader, A.T., Aljeboree, A.M. and A.F. Alkaim (2019). Adsorption and removal of textile dye (methylene blue mb) from aqueous solution by activated carbon as a model (apricot stone source waste) of plant role in environmental enhancement. *Plant Archives*, **19**: 910-914.

Contents

<i>Editorial</i>	i
❑ <i>Snapshots</i>	ii
Life Cycle Assessment of Wastewater Treatment in a Refinery with Focus on the Desalting Process <i>Kouacou Koimbla Francine Josée, Adama Ouattara, Assémian Alain Stéphane and Yao Kouassi Benjamin</i>	1
System Performance Evaluation for Tea Plants Replacing Sprinkler with Drip Irrigation using Water Uniformities in Dooars, India <i>Mantu Das, Subhasish Das and Asis Mazumdar</i>	9
Challenges and Prospects of Flood Early Warning Systems: A Study of Narayani Basin <i>Chandra Lal Pandey and Anoj Basnet</i>	17
IoT Based System for Sewage Overflow Prevention using Heterogeneous Communication Networks <i>Kanchana Rajaram, Mirnalinee, T.T. and Felix Enigo V.S.</i>	25
The Utilisation of International Watercourses from an International Environmental Law Perspective <i>Nanik Trihastuti, Pulung Widhi Hari Hananto and Daniel Rene Kandou</i>	35
Enviro-Health Dimensions of Environment Impact Assessment (EIA) Draft Notification 2020 and COVID-19 Pandemic <i>M.Z.M. Nomani</i>	43
Reduction of Chromium in Waste Water From Hard Chrome Plating Processes: A Review <i>Basavaraja, R.J., Rahul, O., Ranganatha, M., Suhas, K.S. and Vishnumurthy, K.A.</i>	49
Comparative Analysis of Hybrid Photovoltaic Thermal (PV/T) Solar Dryer <i>Sanjay Agrawal, Trapti Varshney and Jitendra Kumar</i>	57
Measurement of Tritium Activity Concentrations in Water Samples of Al-Amara City in Misan Province-Iraq, using Liquid Scintillation Counter <i>Zahraa A. Ismail Al-Sudani, Sawsan S. Fleifil and Mazin Mohammed</i>	67
Synthesis, Characterisation and Utilisation of Magnetic Fe ₃ O ₄ – TGT Nanocomposite in the Removal of Pb(II) from Aqueous Solutions <i>J. Anuradha and N. Muthulakshmi Andal</i>	77
Water Quality Status of the Rivers in Tembilahan City Based on Physical-Chemical Parameters and Storet Index <i>Masykur Hz, Bintal Amin, Sofyan Husein Siregar and Jasril</i>	85
Assessment of Seven Conventional Natural Drinking Water Sources in the Periphery of Chamba Town of Himachal Pradesh in India <i>Tej Singh and Hemant Pal</i>	97
Sustainable Development for Urban Prosperity in Harmony Between Nature and Architecture <i>Adil Hatem Nawar and Ahmed Adnan Saeed</i>	105
Iraq Green Buildings Code Effect on Improving Outdoor Thermal Comfort for Residential Complex <i>Ahmed Kadhim Hado and Susan Abed Hassan</i>	115
<i>Environment News Futures</i>	121